Carbohydrate Polymers 316 (2023) 121079

Contents lists available at ScienceDirect

Carbohydrate Polymers

journal homepage: www.elsevier.com/locate/carbpol

Polyaniline/poly (2-acrylamido-2-methyl-1-propanesulfonic acid) modified cellulose as promising material for sensors design

I. Ragazzini [a], I. Gualandi [a,c,*], G. D'Altri [a], V. Di Matteo [a], L. Yeasmin [a], M.C. Cassani [a,b], E. Scavetta [a], E. Bernardi [a,c], B. Ballarin [a,b,c,*]

[a] Department of Industrial Chemistry "Toso Montanari", Bologna University, UdR INSTM of Bologna, Via Risorgimento 4, I-40136, Bologna, Italy
[b] Center for Industrial Research-Advanced Applications in Mechanical Engineering and Materials Technology CIRI MAM University of Bologna, Viale del Risorgimento 2, I-40136 Bologna, Italy
[c] Center for Industrial Research-Fonti Rinnovabili, Ambiente, Mare e Energia CIRI FRAME University of Bologna, Viale del Risorgimento 2, I-40136 Bologna, Italy

ARTICLE INFO

Keywords:
PANI-PAMPSA
Cellulose
Transducers
Sensors

ABSTRACT

A material based on cellulose coated with polyaniline/poly (2-acrylamido-2-methyl-1-propanesulfonic acid) (Cell/PANI-PAMPSA) was synthesized in a simple way starting from cellulose fibres, aniline and using PAMPSA as dopant. The morphology, mechanical properties, thermal stability, and electrical conductivity were investigated by means of several complementary techniques. The obtained results highlight the excellent features of the Cell/PANI-PAMPSA composite with respect to the Cell/PANI one. Based on the promising performance of this material, novel device functions and wearable applications have been tested. We focused on its possible single use as: i) humidity sensors and ii) disposable biomedical sensors to provide immediate diagnostic services as close to the patient as possible for heart rate or respiration activity monitoring. To our knowledge, this is the first time that Cell/PANI-PAMPSA system has been used for such applications.

1. Introduction

The growing social economic awareness on issues related to the environmental impact and sustainability in the production, use and disposal of goods, strongly encourages the utilization of natural fibre composites for the development of smart materials for various industrial applications (Al-Oqla, Sapuan, Anwer, Jawaid, & Hoque, 2015). In recent decades, cellulose has been used for various highly value-added purposes, such as in the food packaging industry, in the development of innovative batteries, supercapacitors, electrochromic materials and biosensors (Barandun et al., 2019; Fan, Zhang, Li, Yang, & Du, 2020; Seddiqi et al., 2021). Indeed, cellulose has greatly captured the interest of scientists because of its large availability, low density, insolubility in water and in most organic solvents, flexibility and good mechanical properties, non-toxicity, renewability, biodegradability and low-cost (Devabaktuni, Kulkarni, Dixit, Raavi, & Krishna, 2015; Ling et al., 2020; Jung et al., 2015). For several applications cellulose fibres can also derive from recycled cellulose (e.g. from paper or agricultural wastes) (De Haro-Niza, Rincón, Gonzalez, Espinosa, & Rodríguez, 2022; Zhen et al., 2019), furthermore, cellulose-based electronic devices could facilitate the management of their waste streams, as the cellulose part could be recycled or biodegraded to leave recoverable metal constituents (Jung et al., 2015; Sabo, Yermakov, Law, & Elhajjar, 2016).

The production of conductive paper has paved the way for paper electronics (Tobjörk & Österbacka, 2011; Zhang et al., 2018), which on one hand could ease the management of electronic waste by reducing their complexity (i.e. coupling of different materials, including metals) and increasing their recyclability and biodegradability, on the other aspect this would provide innovative solutions in the design of devices not yet commercially feasible, in the field of smart packaging (Grau, Kitsomboonloha, Swisher, Kang, & Subramanian, 2014; Jung et al., 2022), identification tags (Mo et al., 2019; Wang et al., 2019) and wearable devices (Han et al., 2019; Yang et al., 2021). The main strategies are based on the deposition of a thin conductive layer on the paper sheets through screen printing (He et al., 2019), pen-writing (Li et al., 2016), inkjet printing (Raut & Al-Shamery, 2018), spray coating (Say et al., 2020) spin coating (Kim, Moon, & Han, 2004) and vacuum filtration (Hyun, Park, & Chin, 2013) or by combining paper fibres with

* Corresponding authors at: Department of Industrial Chemistry "Toso Montanari", Bologna University, UdR INSTM of Bologna, Via Risorgimento 4, I-40136 Bologna, Italy.
E-mail addresses: isacco.gualandi2@unibo.it (I. Gualandi), barbara.ballarin@unibo.it (B. Ballarin).

https://doi.org/10.1016/j.carbpol.2023.121079
Received 23 February 2023; Received in revised form 26 May 2023; Accepted 29 May 2023
Available online 1 June 2023

conductive materials (Hyun et al., 2013). Carbonaceous nanomaterials (graphene, carbon nanotubes, etc.) play a leading role in the development of these materials (Miyashiro, Hamano, & Umemura, 2020;Parandeh, Kharaziha, & Karimzadeh, 2019; Liu et al., 2019), but at the same time metallic nanomaterials (Nayak, Mohanty, Nayak, & Ramadoss, 2019; Yang, Huang, Payne, Sun, & Wang, 2019) and, especially, conducting polymers have fascinating characteristics (Fei et al., 2019; Fujita et al., 2022; Zhao et al., 2020). Cellulose-based materials show great potential in applications involving conductive polymer composites (Al-Oqla et al., 2015;' He, Tian, Li, Jin, & Li, 2016): PEDOT:PSS [poly(3,4-ethylene-dioxythiophene-poly(styrenesulfonate)] (Fujita et al., 2022), polyaniline (PANI) (Fei et al., 2019) and polypyrrole (PPy) (Zhao et al., 2020) are widely employed in this field. These conjugated polymers exhibit good biocompatibility, but their biodegradability was relatively poor (Liu et al., 2019); a strategy to improve their biodegradability has been to blend them with biodegradable polymers such as cellulose (Liu, Xiang, et al., 2019; Shahadat et al., 2017). For instance, a touch sensor made with PEDOT:PSS inkjet printed on cellulose nanofibril paper resulted to require only 3–4 weeks for a complete degradation in natural soil. It was also possible to recycle it, as the presence of the small amount of PEDOT:PSS ink did not negatively affect the properties of the recycled nano paper (Ling et al., 2020).

Compared to other conducting polymers, polyaniline (PANI) has a unique doping-dedoping mechanism and redox chemical structure. PANI remains one of the most investigated conjugated polymers because of its high electrical conductivity, its multiple electronic states, electrical tuneability, nontoxicity, low manufacturing costs and relative environmental stability (Avelar Dutra, Pires, Nascimento, Mano, & Borges, 2017;' Ke et al., 2019;' Hajlaoui, Khiari, Ajili, Batis, & Bergaoui, 2020). The dopants normally used for doping PANI are small organic or inorganic acids that evaporate at room or higher temperatures, causing a decrease in conductivity in the acid-doped polymers. This drawback can be overcome by using polymeric acid dopants (Yoo et al., 2007; Yoo & Bae, 2013). In addition, polymeric acids with a glass transition temperature (Tg) lower than that of PANI can enhance the flexibility of the polymeric film (Cardoso, Lima, & Lenz, 2007; Yoo et al., 2007; Jeon, O'Neal, Shao, & Lutkenhaus, 2013;' Yoo & Bae, 2013). Consequently, the microstructure of the polymeric acid doped PANI and therefore its properties are expected to be different from those of small size protonic acid-doped ones. Among the polymeric acids, the use of poly (2-acrylamido-2-methyl-1-propanesulfonic acid) (PAMPSA) as dopant allows to improve the properties of the conductive polymer in several ways. Firstly, as shown in Scheme 1, PAMPSA repeating units contain amide groups that can establish additional hydrogen bonding that enhance the water dispersibility of the material. Moreover, as both the monomer and the polymer are strong acids in aqueous solution, they provide the acid environment (pH = 2) that is crucial during aniline polymerization for the formation of the conductive form of PANI. Additionally, PAMPSA preserves the electrical conductivity and improve the flexibility of the final material (Yoo & Bae, 2013; Yoo et al., 2007; Kutorglo et al., 2018; Heller, Feldman, Mano Austin, & Yueh-Lin, 2016; Zhang et al., 2012;' Jeon et al., 2013).

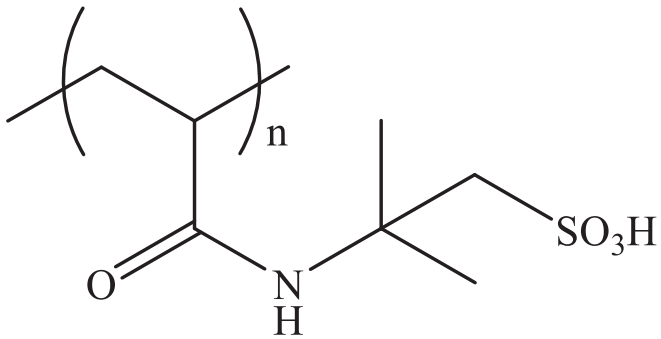

Scheme 1. Chemical structure of PAMPSA.

Finally, it is known that the conductivity of PANI-PAMPSA depends on the molecular weight of the PAMPSA template. More specifically, the conductivity increases monotonically with the decreasing of PAMPSA molecular weight, ranging from 0.4 to 1.1 S cm^{-1} for a PAMPSA that is lower than 800 Kg mol^{-1} (Heller et al., 2016; Zhang et al., 2012).

Our group has recently investigated conductive polymer composites based on cellulose fibres coated with polyaniline (Cell/PANI) (Ragazzini et al., 2021; Ragazzini et al., 2022). This conductive paper was employed in the preparation of resistive and humidity touch sensors (Ragazzini et al., 2021; Ragazzini et al., 2022). Despite the good performances obtained in both cases, critical issues were represented by the poor mechanical stability and flexibility of the final composite materials, characteristics that are crucial for real applications in the field of paper electronics (Chen et al., 2022;' Muralee Gopi, Vinodh, Sambasivam, Obaidat, & Kim, 2020). To improve these qualities and increase the biocompatibility of the conductive polymer composite for applications in close contact with the skin (Bayer, Trenchard, & Peppas, 2010), we have now prepared a Cell/PANI-PAMPSA composite. Moreover, PAMPSA seems to provide self-healing features to tactile sensors, an important ability to reduce electronic waste in long-term applications (Bubniene, Ratautaite, Ramanavicius, & Bucinskas, 2022).

The Cell/PANI-PAMPSA composite has been synthesized in a simple way starting from cellulose fibres, PANI and using PAMPSA as dopant. The morphological features, mechanical properties, thermal stability and electrical conductivity highlight the excellent properties of the Cell/PANI-PAMPSA composite. Based on the promising performance of the materials, novel applications have been tested. In particular, we focused on their possible single use as: i) humidity sensors and ii) biomedical sensor for heart rate or respiration activity to provide rapid diagnostic tools that operate as close to the patient as possible. To our knowledge, this is the first time that Cell/PANI-PAMPSA has been used for such applications.

2. Materials and methods

2.1. Materials

All chemicals and solvents are ACS reagent grade and were purchased from commercial vendors and used directly unless otherwise stated. Sulfuric acid (H_2SO_4, 95.0–98.0 %), ammonium persulfate [APS, $(NH_4)_2S_2O_8$), ≥ 98 %] and aniline (≥ 99 %), were purchased from Sigma-Aldrich (now Merck KGaA, Darmstadt, Germany); aniline was distilled under nitrogen prior to use. Chloridric acid (≥ 37 %) was purchased from VWR Chemicals (Vienna, Austria); a solution of ca. 25 wt% of $Al_2(SO_4)_3$ in water (commercial name FLOCLINE S8C) was purchased from Bio-Line s.r.l. (Milano, Italy). Poly (2-acrylamido-2-methyl-1-propanesulphonic acid) (PAMPSA), MW ~ 800,000, 10 wt% aq. sol. Was purchased from Acros Organics. Universal pH paper test was purchased by Jovitec. Bare cellulose fibres (pine tree long fibre with sulfate treatment) and recycled cellulose fibre (Cellrec) were kindly provided by Cromatos s.r.l. (https://www.cromatos.com/, Forlì, Italy).

2.2. Cell/PANI-PAMPSA synthesis

In a 1.0 L round bottom flask, 2.5 g of bare cellulose fibres were dispersed in demineralized water (300 mL) for 30 min, then 2.54 mL of aniline and 58.0 g of PAMPSA were added to the fibre suspension and stirred for 1 h at room temperature (Yoo et al., 2007). Successively, 5.8 g of APS was dissolved in 25 mL of distilled water, with a fixed aniline to APS molar ratios of 1 (Yoo & Bae, 2013). The APS solution was slowly added dropwise to the stirred suspension containing aniline, PAMSA and cellulose, the flask was kept at 0 °C in an ice bath for 6 h. After 24 h the coated fibres were filtered in a Buchner funnel and washed several times with 1.0 M citric acid solution. The conductive fibres (Cell/PANI-PAMPSA or Cellrec/PANI-PAMPSA) were dried in air atmosphere for 24

h. To obtain a 0.20 mm thickness sheet, 5.0 g of conductive fibres were added to 1.0 L of demineralized water and stirred for 5 min and then the fibres were partially dried in a square sieve (21.0 cm × 14.8 cm size, typical A5 paper format). Finally, the sheet was pressed at 50 bar pressures (P50 AXA manual hydraulic press) for 10 s. The thickness of the sheet is different and can be varied by changing the amount of modified cellulose that is used (i.e., 10 g for 0.40 mm, etc.). For comparison, Cell/PANI sheets were prepared as previously reported (Ragazzini et al., 2021).

2.3. Fabrication of the sensors

2.3.1. Humidity sensors

To increase the mechanical resistance of the conductive sheets, we employed the industrially wet coupling method already used for Cell/PANI (Ragazzini et al., 2021). Briefly, a Cell/PANI-PAMPSA sheet of 0.20 mm thickness was coupled with a bare cellulose sheet (thickness 0.20 mm), previously moistened with water. The two sheets were then pressed (50 bar, 10 s) and dried at 80 °C for 10 min. Finally, the sensors were prepared by cutting from the sheets a rectangle of 2.2 × 0.9 cm in size. The active material is connected to the instrument with two copper wires endowed with two alligators placed on the two extremities of the rectangle.

A cooling incubator with controlled humidity (climatic chamber, ClimaCell 111 comfort, MMM Group), equipped with humidity and temperature sensors for controlling the climatic chamber operating conditions, has been used to obtain an exact and reproducible simulation of variable climatic conditions (i.e., %RH). The tests have been carried out at a fixed temperature of 21 ± 1 °C. The responses of Cell/PANI humidity sensor were acquired with a potentiostat/galvanostat by applying a potential of 0.100 V and recording the current that flows in the material. During the tests, the humidity was changed with a set step uphill (5 %) from 30 % up to 50 %RH, and each step was maintained for 1 h and 15 min (total time for each measure: 7.5 h) (Fig. S1, SI).

Finally, a further commercial digital-output relative humidity & temperature sensor was used to monitor and record the %RH and temperature inside the climatic chamber during each test. Among the low-cost sensors available on the market the DHT22 (also named AM2302, Guangzhou Aosong Electronics Co., Ltd., China, temperature from −40 to +80 °C +/− 0.5 °C and relative humidity from 0 to 100 % +/− 2.0 %, prize 9.9 USD) was chosen because can be calibrated in an extremely precise manner, and it is compatible with Arduino data collection system.

Using Eq. (1) and the parameters of the linear curves obtained with Cell/PANI-PAMPSA sensors, it is possible to transform the current signal into a %RH signal, for directly comparing the response with those of DHT22.

$$RH\%signal = \frac{i(\mu A) - intercept(\mu A)}{slope\left(\frac{\mu A}{RH\%}\right)} \quad (1)$$

In order to compare the humidity sensitivity between different sensors, the current signal was expressed as the normalized response, which is defined as Eq. (2) (Jain, Chakane, Samui, Krishnamurthy, & Bhoraskar, 2003; Zhao et al., 2017):

$$\frac{\Delta S}{S_0}\% = \frac{S - S_0}{S_0}\ 100 \quad (2)$$

where S_0 is the signal of the sensor at the start %RH and S stands for the signal at targeted %RH environment. All the measurements were performed in triplicate with three different sensors.

2.3.2. Biomedical sensors

Cell/PANI-PAMPSA was applied for monitoring various physiological signals such as heart rate and respiratory activity. For heart rate (EGC measurements) two square Cell/PANI-PAMPSA electrodes with dimensions of 2.0 cm^2 were cut from the original A5 sheet and connected to the potentiostat with two copper wires endowed with two alligators (Scheme 2B). The electrodes were moistened before applications and were positioned as shown in Scheme 2A. To acquire the ECG graph, the instrument monitored the difference of potentials between the electrodes in the time. The experiments were carried out being careful on avoiding the electrical contact between the metal elements and the skin. All the measurements were repeated three times using three different couples of electrodes. An ECG graph that represents the usual output is reported in the Result and discussion section.

As regards the respiratory behaviour monitoring, a Cell/PANI-PAMPSA rectangular sensor with dimensions of 5 cm^2 (1 × 5 cm) was proceeded from the original A5 sheet and inserted between a FFP2 and FFP1 face mask, as shown in Scheme 3 and Fig. S2, and then connected with the potentiostat with two copper wires endowed with two alligators. The current vs time curves were registered during a normal respiratory activity while a fixed potential was applied between the two extremities of rectangular active material (0.1 V, interval time 0.1 s). All the measurements were performed in triplicate using different sensors for each measure.

2.3.2.1. Instruments. SEM images were recorded at 25 kV with a SEM Zeiss EVO 50 EP equipped with Oxford INCA 350; EDS Spectrometer equipped with a Bruker Z200 energy dispersive microanalysis (EDX) system was used for semi-quantitative chemical analysis and mapping. TGA characterization was carried out using a Perkin Elmer TGA-7 instrument. In each analysis, a piece of weight ca. 4.0 mg of the target sample was heated in a platinum crucible from 38 °C to 950 °C (or 800 °C for cellulose), at a rate of 10 °C min^{-1}, under N_2 atmosphere. ATR-FTIR analyses were performed using a Perkin Elmer Spectrum Two spectrophotometer, equipped with a Universal ATR accessory, with a resolution of 0.5 cm^{-1} in the range 4000–400 cm^{-1}. The samples were directly analyzed performing 40 scans for each analysis. The chronoamperometric measurements were performed using a potentiostat/galvanostat Autolab PGSTAT128N (Metrohm-Autolab) controlled by NOVA 2.10 software. A cooling incubator with controlled humidity (climatic chamber, ClimaCell 111 comfort, MMM Group) was used for the humidity tests at a fixed temperature of 21 ± 1 °C following the chronoamperometric response of the humidity sensor at an applied potential of 0.100 V. For the tests with Cell/PANI-PAAMPSA sensors we set steps uphill (5 %) from 30 % up to 50 % RH, and each step was maintained for 1 h and 15 min (total time for each measure: 7.5 h). For comparison, a commercial digital-output relative humidity & temperature sensor/module DHT22 was used to monitor the % RH and temperature inside the climatic chamber. Tensile strength measurements have been carried out on a LBG UDI24Pro Instrument with a traction speed of 1 mm min^{-1}. The samples have been prepared following the TAPPI method reported in the literature by cutting the different sheets (cellulose, recycled cellulose, Cell/PANI, Cell/PANI-PAMPSA, Cellric/PANI and Cellrec/PANI-PAMPSA) into rectangles with a central size of 2.0 × 10.0 cm, 0.4 mm of thickness and 1.5 cm for each side for the crimping points (Muchorski, 2006).

3. Results and discussion

3.1. Characterization

The conductive paper was prepared using cellulose fibrils covered with a thin film of PANI/PAMPSA obtained through the in-situ polymerization of aniline. This procedure has been developed by our research group for the production of sheets of conductive paper based on Cell/PANI (Ragazzini et al., 2021; Ragazzini et al., 2022). The reaction is carried out under mild conditions at 0 °C and under atmospheric pressure.

The SEM characterization (Fig. 1) shows that the synthesis leads to

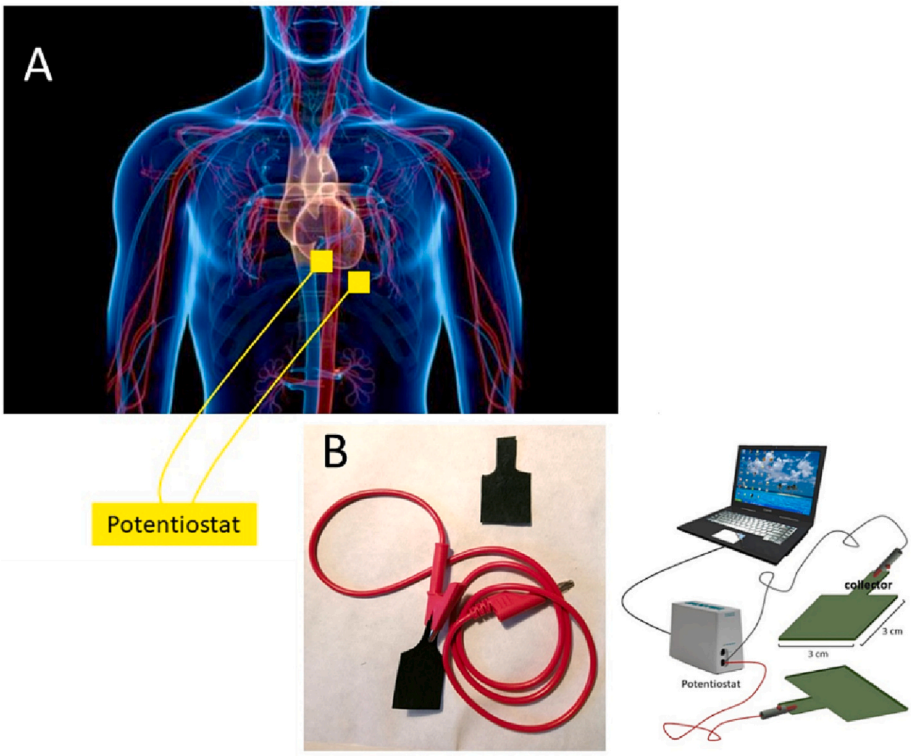

Scheme 2. A) Cell/PANI-PAAMPSA sensors position for EGC measurements; B) Cell/PANI-PAMPSA sensors and potentiostat connection.

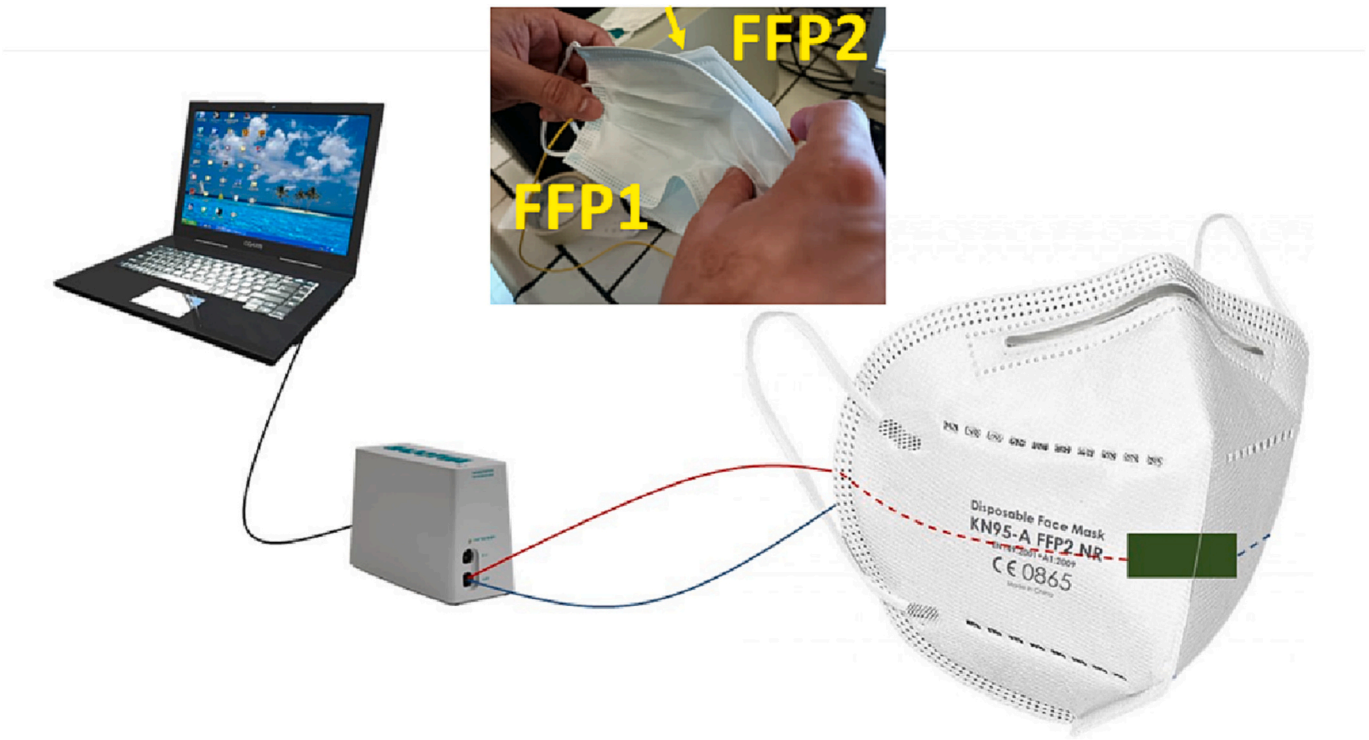

Scheme 3. Respiratory behaviour measurements.

the formation of a uniform and continuous film of PANI/PAMPSA on the surface of the cellulose fibrils (Fig. 1B). The polymer consists of small particles, with dimensions close to the resolution of the instrument, which are not present in the image recorded for cellulose alone (Fig. 1A). At the same time the PANI/PAMPSA coated cellulose appears less fibrous than the cellulose in its original structure. Finally, the images recorded for Cell/PANI-PAMPSA are similar to those obtained for Cell/PANI (Fig. 1C), showing that the presence of PAMPSA does not alter the morphology of the modified cellulose. The conductive sheets were made by exploiting a traditional method for paper production as described in §

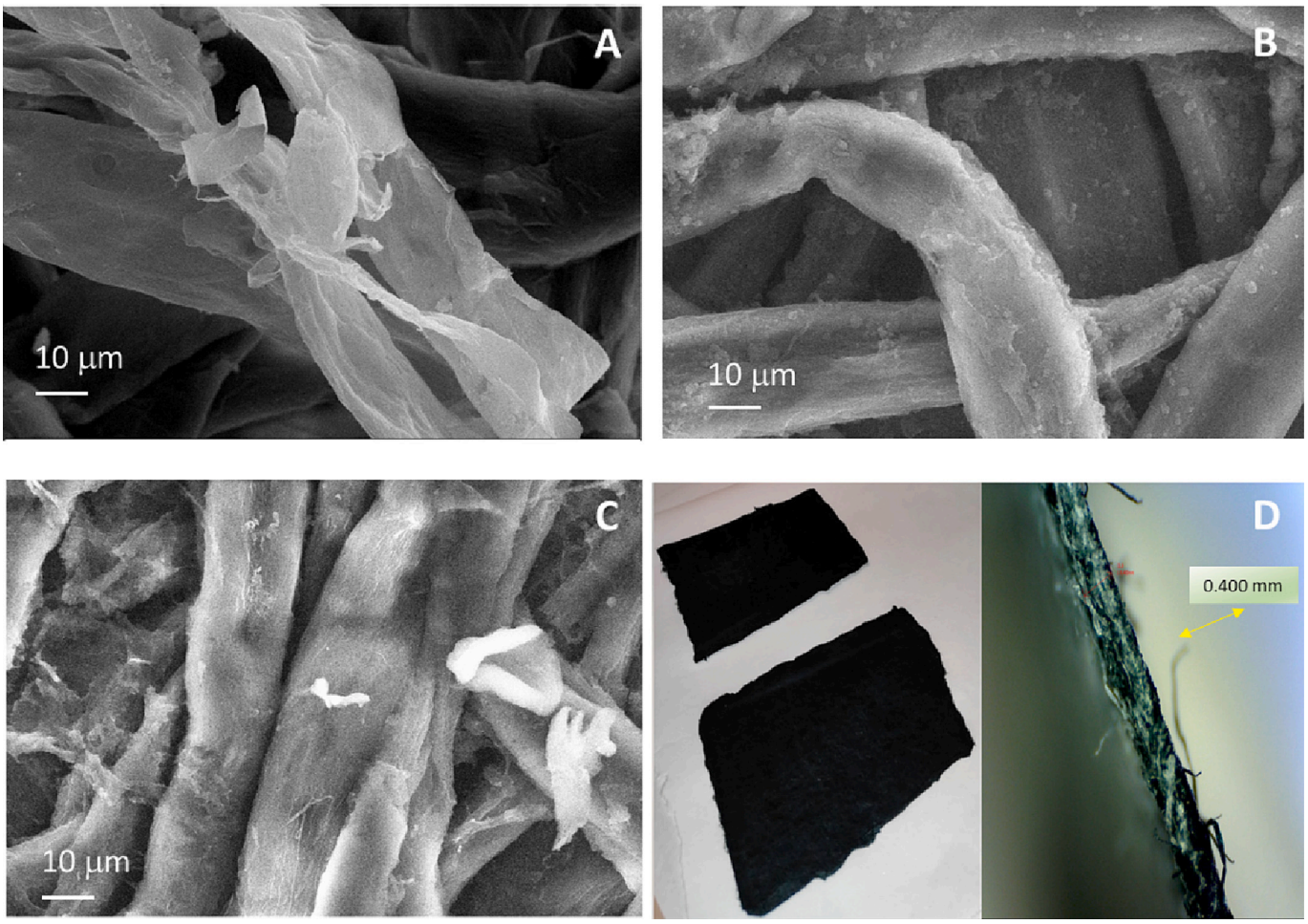

Fig. 1. SEM micrograph of: A) pristine cellulose; B) Cell/PANI-PAMPSA; C) Cell/PANI; D) image of the final paper sheets and cross-section of Cell/PANI-PAMPSA.

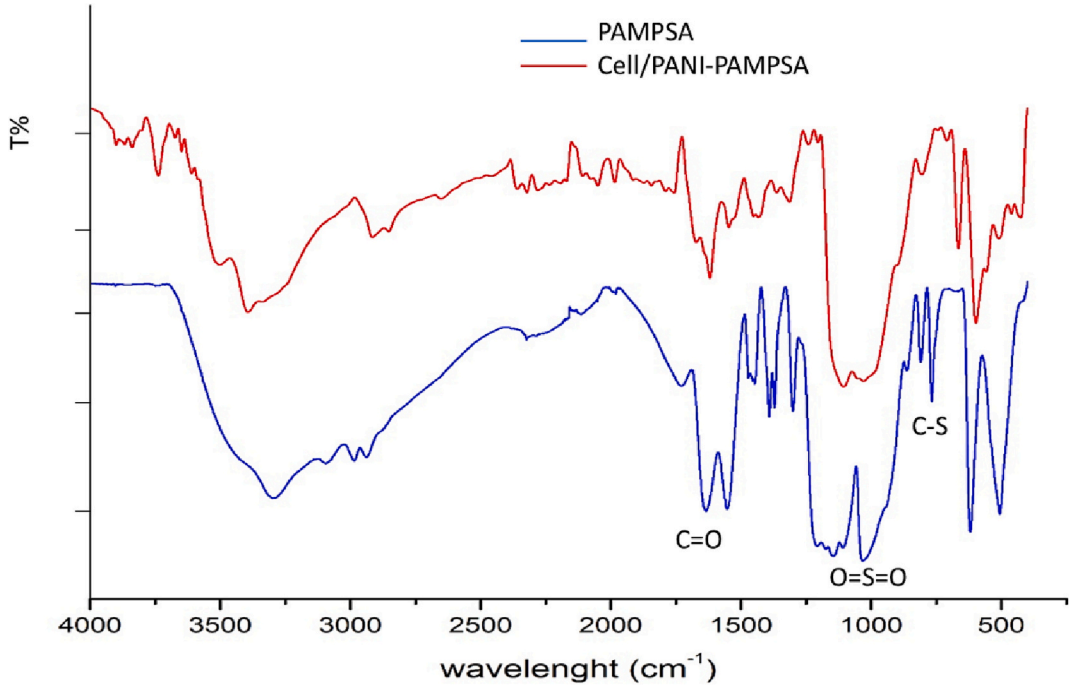

Fig. 2. ATR-FTR spectra of Cell/PANI-PAMPSA (red line) and PAMPSA (blue line).

2.2, Cell/PANI-PAMPSA fibres were first dispersed in water, then partially dried in a square sieve and finally pressed.

The paper sheets made of Cell/PANI-PAMPSA (Fig. 1D, and § 2.2), exhibit good flexibility and appear much more resistant than the sheets prepared with Cell/PANI (see §3.3). These excellent results suggest a possible rapid industrialization as the fibrils modified with PANI-PAMPSA behave as the bare cellulose fibrils. The success of the modification with PANI-PAMPSA has also been demonstrated by an investigation with IR spectroscopy, which clearly shows the characteristic patterns of both components of the polymeric blend.

Fig. 2 shows the ATR-FTIR spectra with the characteristic absorption peaks for PAMPSA and Cell/PANI-PAMPSA. In the Cell/PANI-PAMPSA, the strong bands located at approximately 1650 cm^{-1} and 1032 cm^{-1} are respectively attributed to the C═O and the symmetric O=S=O stretchings, which correspond to the carbonyl and sulfonic groups of PAMPSA (Gribkova et al., 2013; Shen et al., 2018). The bands at 1296 cm^{-1} and 1148 cm^{-1} are assigned to the protonated amine and protonated imine groups respectively (Shen et al., 2018). Other bands are observed at 923 cm^{-1} (S − O stretching), and 795 cm^{-1} (C − S stretching and C − H out-of-plane bending) (Heller et al., 2016), 1302–1304 cm^{-1}, 1243–1245 cm^{-1}, 1108–1119 cm^{-1} for the PANI emeraldine salts (Pang et al., 2016; Rahayu et al., 2019; Yoo & Bae, 2013). Finally, the bands of quinoid and benzenoid observed at 1546 cm^{-1} and 1440 cm^{-1} suggest an interaction between the backbone of PANI and PAMPSA which is associated with the p-electron delocalization induced by protonation (Shen et al., 2018).

In summary, the in-situ synthesis procedure covers the cellulose fibrils with a uniform film of PANI/PAMPSA as highlighted by the SEM and IR characterizations.

The TGA curves of the Cell/PANI-PAMPSA, Cell/PANI and pristine cellulose are reported in Fig. S3. Due to the highly hygroscopic nature of cellulose and polyaniline, the first stage of mass loss (about 5 %) up to 160–180 °C can be ascribed to the loss of water. The second stage which starts at around 160 °C (with a lower loss in the case of PANI-PAMPSA: 57.6 vs 65.2 % for PANI) is due to loss of dopant and low molar mass oligomers, cross-linked fragments of chains and the initiation of polymer degradation. The last stage of mass loss that occurs at around 500 °C corresponds to the total rupture of polymer bonds (polyaniline and cellulose), as well as heavier fragments in even smaller fractions and gaseous by-products. The residues remaining at 900 °C for Cell/PANI-PAMPSA (24.3 %) are inert materials, such as fragments of carbonized polymer chains (Nepomuceno, Seixas, Medeiros, & Mélo, 2021).

Cell/PANI shows a higher mass variation at 160 °C suggesting the material loses the dopant during this stage. Since HCl is the main dopant species, acid release tests we conducted on Cell/PANI-PAMPSA in a closed chamber in the presence of a pH tester paper for 72 h; the results have then been compared with those obtained with Cell/PANI. As observable in Fig. S4 in proximity to Cell/PANI, the pH tester paper turns in red colour in about 48 h indicating an acid release whereas no change in colour occurs with Cell/PANI-PAMPSA exposure. These data highlight the better biocompatibility of Cell/PANI-PAMPSA than Cell/PANI.

3.2. Mechanical and electrical properties

The synthesis approach described in the previous paragraphs has already been investigated to produce sheets based on Cell/PANI alone. Therefore, it is important to identify the role that PAMPSA plays in defining the technological properties of conductive paper.

To better investigate the mechanical properties of the materials, the tensile strength of the Cell/PANI-PAMPSA sheets has been measured and compared with Cell/PANI and pristine Cellulose. The results reported in Table 1 and Fig. 3 are the average of the measures carried out for three different samples for each type of material.

Differently from the acidic media used for Cell/PANI preparation, the use of PAMPSA during the cellulose fibres modification does not damage the fibres and improves the mechanical properties of the modified cellulose, resulting in a tensile strength that is more than three times higher compared to Cell/PANI. Reasonably, the hydrogen bonds and electrostatic interactions between PAMPSA and PANI build up a homogeneous dynamic network, which contributes to the elasticity and soft compliant nature of the as-prepared electronic polymer material with high omnidirectional stretchability (Boland et al., 2014; Kim et al., 2015; Seyedin, Razal, Innis, & Wallace, 2014; Wu, Li, An, & Sun, 2016).

Table 1
Tensile strength values obtained from mechanical tests for pristine Cellulose, Cell/PANI and Cell/PANI-PAMPSA.

Sample	Stress at break (MPa)	Strain at Break (%)
Cellulose	0.0094 ± 0.0008	20 ± 5
Cell/PANI	0.0040 ± 0.0009	9.8 ± 0.5
Cell/PANI-PAMPSA	0.016 ± 0.003	52 ± 5

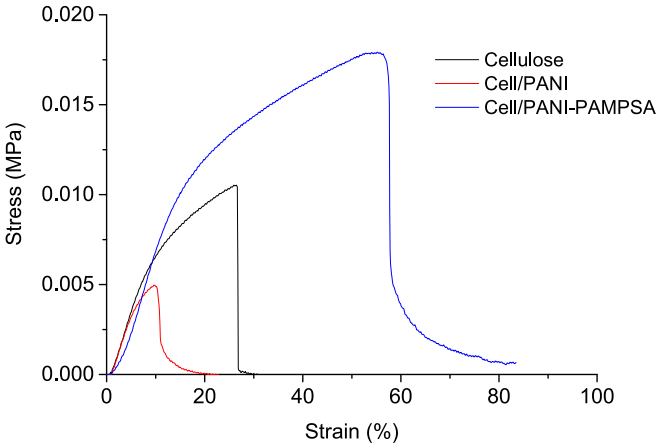

Fig. 3. Stress-strain curves obtained for pristine Cellulose (black line), Cell/PANI (red line) and Cell/PANI-PAMPSA (blue line).

Cell/PANI and Cell/PANI-PAMPSA electrical conductivities were measured with a Keysight B2902A source meter units in a 4-line-probe configuration by exploiting a home-made holder that is composed of 4 parallel copper electrodes on a glass slide (Fig. S5). The data reported in Table 2 represent averages from five measurements each.

As expected, the conductivity of Cell/PANI-PAMPSA is lower than that of Cell/PANI because PAMPSA is inherently insulating; an excess of PAMPSA can thus hinder charge hopping and macroscopic conduction nevertheless, the values obtained are still suitable for sensor applications.

Moreover, the flexible properties of a material are very important for applications such as wearable sensors or energy storage devices (Wang et al., 2021; Seshadri et al., 2019;' Heikenfeld et al., 2018). To study the flexible behaviour of Cell/PANI-PAMPSA in comparison with Cell-PANI, a homemade 3d-printed support is built to fold pieces of paper in a reproducible way (Fig. S6). The conductivity of Cell/PANI-PAMPSA was measured with a 4-probe tester before and after a series of foldings and was compared with those of Cell/PANI.

As reported in Fig. 4, the conductivity of Cell/PANI decreased progressively (39 %) under the folding and the material broke after 200 foldings (Fig. S7). On the contrary, the conductivity of Cell/PANI-PAMPSA decreased by only 16 %, and the sheets start to break after

Table 2
Conductivity values for Cell/PANI and Cell/PANI-PAMPSA.

Samples	S cm^{-1} (*10^{-1})
Cell/PANI	3.45 ± 0.01
Cell/PANI-PAMPSA	0.537 ± 0.001

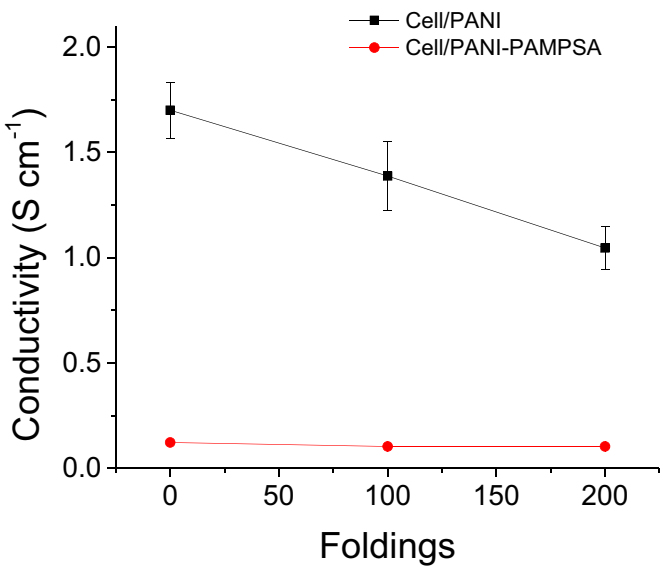

Fig. 4. Conductivity graphs vs folding number for (■black) Cell/PANI and (● red) Cell/PANI-PAMPSA during the bending test. Error bars for Cell/PANI-PAMPSA are negligible.

500 foldings.

In summary, PAMPSA improves the mechanical properties of paper and preserves the electrical properties after repeated mechanical deformations. Conversely, the introduction of PAMPSA which is an insulating polyelectrolyte, leads to a worsening of the electrical conductivity when compared to that of sheets obtained with Cell/PANI.

3.2.1. *Mechanical and electrical properties of recycled cellulose*

To check the possibility to employ recycled cellulose, Cellrec/PANI and Cellrec/PANI-PAMPSA samples have been prepared and characterized in terms of mechanical stability and conductivity. In recycled paper, (Han, Zhang, Hoang, Gray, & Xie, 2021; Izadi, Hosseini, Najafpour Darzi, Nabi Bidhendi, & Pajoum Shariati, 2018) the cellulose fibres are very short and this feature leads to a decrease in the mechanical stability of the final paper sheet. This problem is evident if we compare the stress/strain curves reported in Fig. S8 for cellulose and recycled cellulose. The addition of PAMPSA in the modified recycled cellulose gives an improvement in mechanical stability as clearly visible in the stress-strain curves reported in Fig. S9 and in data shown in Table S1. The electrical conductivities measured with a 4-line-probe configuration of Cellrec/PANI-PAMPSA results like those of Cell/PANI-PAMPSA (0.501 ± 0,001 S cm^{-1} *10^{-1}) pointing out that the cellulose recycling does not affect the performance of the modified fibres.

3.3. *Device applications*

The Cell/PANI-PAMPSA exhibits very fascinating properties to be used as materials for paper electronics. The Cell/PANI has been already used for producing all-paper touch and humidity sensors, but its fragility and acid release could hinder its widespread use. The mechanical strength and high biocompatibility (Bayer et al., 2010) of Cell/PANI-PAMPSA make it a promising material for these applications, but further experiments are needed to underpin its real use, considering the decrease of electrical conductivity due to the introduction of an insulating polymer into the material. To demonstrate its superior properties, we fabricated, employing only pristine cellulose as starting material, humidity and breath sensors and electrocardiogram electrodes.

3.3.1. *Humidity sensing*

With the aim to compare the sensing behaviour of Cell/PANI-PAMPSA with that of Cell/PANI (Ragazzini et al., 2022) by employing a method commonly used in the paper industry, we coupled the Cell/PANI-PAMSA sheet with a bare cellulose sheet (thickness 0.40 mm) previously moistened with water. The two sheets were then pressed (50 bar, 10 s, final thickness of 0.80 mm) and dried at 80 °C for 10 min. Then the humidity sensor is prepared by cutting out the sheet of Cell/PANI-PAMPSA of rectangular shape usually of dimensions 2.2 × 0.9 cm^2 at the ends of which a potential of 0.100 V is applied. The current flowing in the material is the signal used by the sensor. As reported in literature (Sezen-Edmonds, Yeh, Yao, & Loo, 2019), the increase in the conductivity of PANI-PAMPSA with humidity is ascribed to the increased solvation of the polymer acid with water exposure. Moreover, since conducting PANI is preferentially located on the exterior of PANI-PAMPSA globules, swelling of PAMPSA with water absorption should not disrupt the connectivity of the conducting domains; it should instead bring the conducting domains closer (Sezen-Edmonds et al., 2019). The performance as a sensor was evaluated in a climatic chamber wherein the humidity value was varied in a controlled way. Moreover, for comparison, the humidity sensor DHT22 was used to monitor the humidity level during the experiments.

The current vs time curves for Cell/PANI-PAMPSA and % RH vs time curves registered with DHT22 are reported in Fig. 5; the oscillation in the signal, observed with all the sensors employed are due to the fluctuations present in the chamber for each % RH variation. Indeed, when necessary, inside the chamber the climatic parameters are iteratively adjusted through heating/cooling and humidification/dehumidification processes to maintain the temperature and % RH values as faithful as possible to the programmed ones. Beyond the device studied in this paper, the experimental setup is endowed with a double system for monitoring the humidity level (DHT22 and climate chamber sensor).

From the response values obtained (considering the values in the middle of the plateau registered for each step), it is possible to calculate the current vs % RH response curves (Fig. S10) that present a linear trend ($y = 0.11\times + 10.28$, $R^2 = 0.996$). The slope results about one order of magnitude lower than that observed previously with Cell/PANI (0.11 vs 1.41 μA/%RH respectively) in agreement with the lower Cell/PANI-PAMPSA conductivity (Ragazzini et al., 2022). From Eq. (1) (§2.3.1) it is possible to transform the current signal into an RH% signal and directly compare the response of Cell/PANI-PAMPSA with those of the DHT22 sensor, as reported in Fig. 6.

A perfect overlap of the two signals was observed. In order to compare the humidity sensitivity between Cell/PANI-PAMPSA, Cell/PANI and DHT22, the normalized response, which is defined in §2.3.1 (Jain et al., 2003; Zhao et al., 2017), was calculated. The responses vs RH% relationship is reported in Fig. 7; Cell/PANI-PAMPSA present a good linearity ($R^2 = 0.998$) in the RH% range investigated.

The slopes of the curves for Cell/PANI-PAMPSA (3.3 ± 0.1), Cell/PANI and DHT22 (3.3 ± 0.1 and 3.44 ± 0.03, respectively) show that the rate of change response of the three sensors is statistically equal. The data suggest the good humidity sensing performance of Cell/PANI-PAMPSA.

3.3.2. *Biomedical sensing – respiratory behaviour*

Breathing patterns contain fundamental information (rate, depth, and rhythm) that represent the most informative vital signs. In healthcare, variations in respiratory frequency can be used as predictors of physiological deterioration and serious adverse events. In sports and physical activities, respiratory frequency is a valid marker of physical effort and is associated with exercise tolerance in different populations (Al-Halhouli et al., 2021; Kano et al., 2022; Piuzzi, Pisa, Pittella, Podestà, & Sangiovanni, 2020). For example, the respiratory rate is 10–20 breaths per minute (bpm) for a healthy adult whereas an abnormal respiratory rate (< 6 bpm or > 24 bpm) is a prediction of mortality heart rate or hypertension; on the contrary with a high-intensity exercise, the respiratory rate can become as high as 60 bpm (Duan, Jiang, & Tai, 2021). Despite various sensors, such as flexible pressure, strain, temperature and Fibre Bragg Grating (FBG) sensors

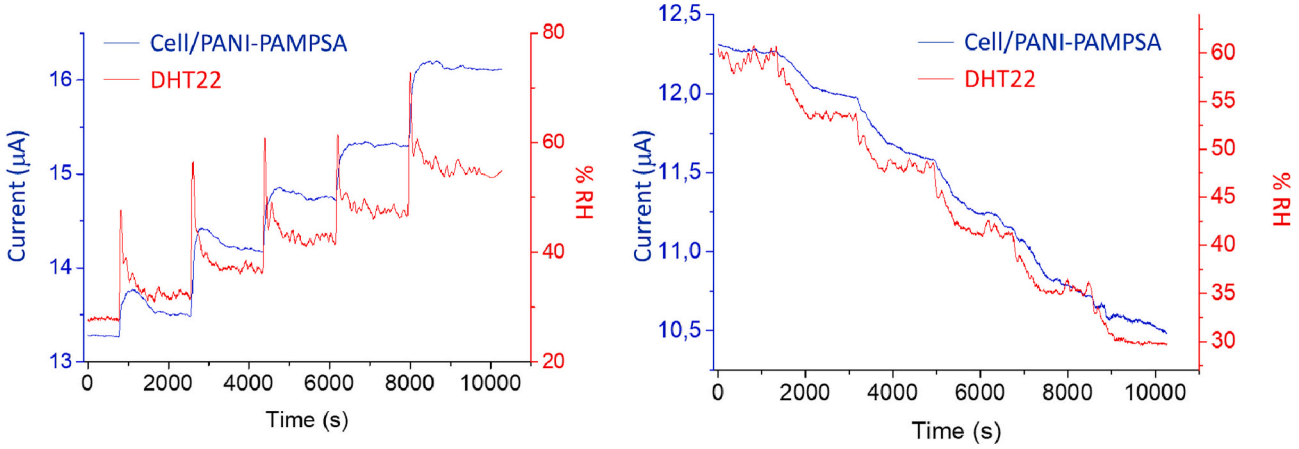

Fig. 5. Current vs time curves registered uphill and downhill for Cell/PANI-PAMPSA (blue line) and DHT22 (red line).

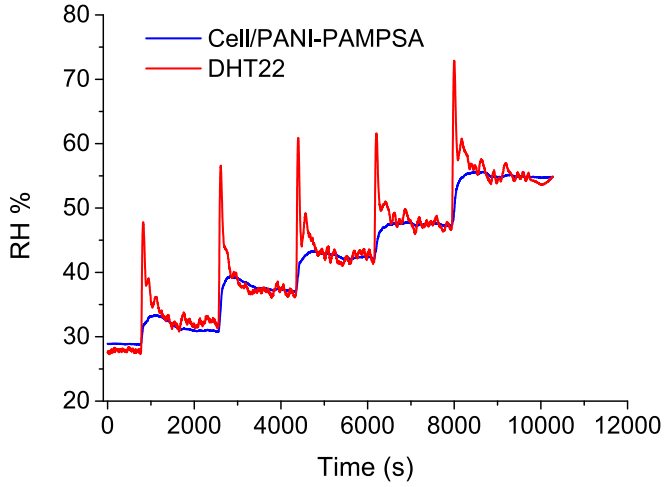

Fig. 6. Comparison between the response of Cell/PANI-PAMPSA (blue line) and DHT22 (red line) under pulse stimuli obtained by switching between 30 and 55 % RH in a climate chamber. The test was carried out using an applied voltage of 0.100 V at 21 ± 1 °C.

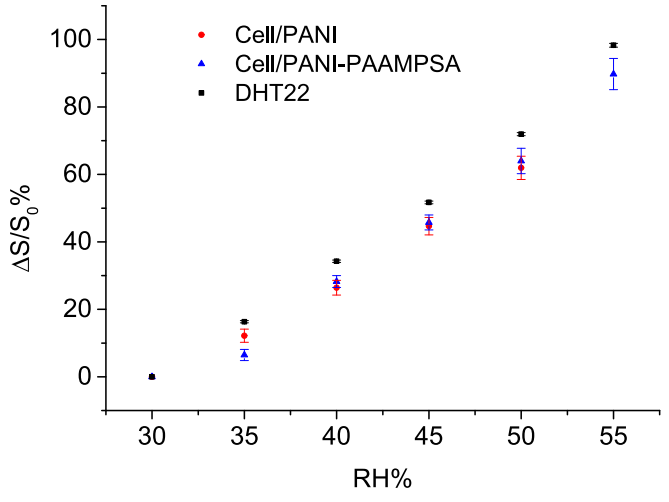

Fig. 7. Response vs RH% relationship of Cell/PANI-PAMPSA (y = 3.30 x − 101.09, R^2 = 0.998) (▲ blue), Cell/PANI (y = 3.34 x − 102.10, R^2 = 0.998) (● red) and DHT22 (y = 3.44 x − 103.31, R^2 = 0.999) (■black) sensors. All the measurements were performed in triplicate.

(Duan et al., 2021), have been used until now, often they fail in terms of stability, accuracy or cost.

The humidity sensors exhibit a large response/recovery rate making them ideal candidates for respiratory detection (Kano et al., 2022). A rectangular Cell/PANI-PAMPSA sheet with dimensions of 5 cm^2 (1 × 5 cm), has been embedded between an FFP2 and FFP1 face mask and has been fixed using a pointer as shown in Scheme 3 and Fig. S2 to be used as a breath sensor. The fabrication process is very simple and easily integrable in a mass production plant. A fixed potential is applied between the two extremities of the sensor, and the signal is the current flowing in the material.

In Fig. 8 we present the response curve for nose breathing rate obtained interspersing 30 s without breathing (A) with normal (B) or fast (C) breathing. The data are reported without processing the signal, normally necessary to eliminate the baseline drift of the respiratory rate response curve (Duan et al., 2021). In the absence of breathing, the signal is flat, in accordance with a stable humidity value inside the mask. Instead, during respiration, the current value fluctuates due to the humidity variation generated by breath. Greater is the intensity of breathing, greater is the signal oscillation. The data shows that the sensor can measure the respiratory rate by also identifying the intensity of respiration.

3.3.3. *Biomedical sensing – ECG measuring*

Bioelectric signals coming from the human body could give important information about physiological functions and routine healthcare,

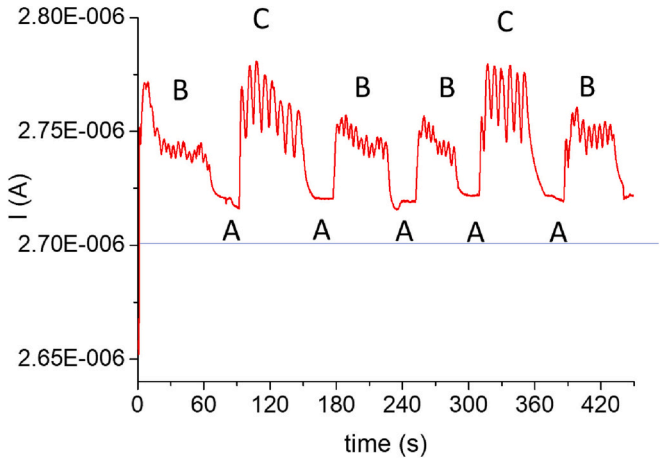

Fig. 8. Response curve for noise breathing rate; A) 30 s without breath; B) 60 s normal breath; C) 60 s fast breath.

therefore they have been widely studied to provide immediate diagnostic and therapeutic services (Chen et al., 2022;' Acar et al., 2019). One of the most investigated technologies in this field is the Electrocardiogram (ECG) that, collecting bioelectrical signals with electrodes on the surface of the body, could give not only a clinical diagnosis of various heart diseases, but also represent a simple but effective tool to explain arrhythmia and conduction disorders (Ankhili, Tao, Cochrane, Coulon, & Koncar, 2018; Shathi, Chen, Khoso, Rahman, & Bhattacharjee, 2020;' Yamamoto et al., 2017;' Yapici & Alkhidir, 2017). ECG sensors detect the polarization and depolarization of myocardial cells that generate electric current (Al-Ani, 2018). An important criterion for suitable electrodes is low impedance to limit the noise generated during signal recording. The stratum corneum (SC), which is the top layer of the skin, has a high impedance, so the application of a gel that hydrates the SC is necessary to create an ionic path between the metal part of the electrode and the skin allowing a good contact during body movement (Webster, 2010;'Ankhili et al., 2018). Unfortunately, conductive gel sometimes causes allergic symptoms on the skin and can dry in a short time causing noise in the electrical signals; to overcome this problem textile electrodes manufactured from common fabrics treated with conductive polymers have been recently studied (Acar et al., 2019; Castrillón, Pérez, & Andrade-Caicedo, 2018; Yamamoto et al., 2017). Cell/PANI-PAMPSA can be a valid replacement due to its high sensitivity, biocompatibility, flexibility, mechanical stability, and low cost, as well as more sustainable disposal compared to conventional AgCl gel electrodes. Two square Cell/PANI-PAMPSA electrodes (2.0 × 2.0 cm) were placed on the skin close to the heart (Scheme 2), and the difference in voltage between the two electrodes was measured. Due to the conductive form of PANI-PAMPSA, it is not necessary the use of a conductive gel and the two square electrodes can be directly positioned after being moistened. Fig. 9 shows the ECG output registered on a volunteer with a normal sinus rhythm. The three main components of a typical ECG tracing can be recognized: the P wave, which represents depolarization of the atria, the QRS complex, which represents depolarization of the ventricles and the T wave which represents repolarization of the ventricles. Furthermore, it is possible to measure the RR interval which represents the time elapsed between two successive R-waves of the QRS signal on the electrocardiogram and to see the U wave which represents the last phase of ventricular repolarization.

4. Conclusions

The synthesis of new materials for paper electronics plays a key role in the creation of biocompatible, eco-friendly, biodegradable, recyclable and low-cost devices, which can also be exploited to develop gadgets that are not yet commercially available. The intimate modification of cellulose fibrils with polyaniline has proven to be an attractive approach to produce conductive paper sheets that have been exploited in the fabrication of touch and humidity sensors. However, the fragility and the slow acid release hinder their effective use in a real environment. The introduction of PAMPSA, used as a polyelectrolytic dopant, increases the mechanical resistance of the material and makes the material biocompatible because of the replacement of the HCl dopant. The excellent properties of metal-free Cell/PANI-PAMPSA sheets have been demonstrated by realizing proof of concept biomedical devices based on this material by successfully building electrocardiogram electrodes, without using any electrode gel, and humidity sensors. The integration of the humidity sensor inside a mask allows the monitoring of the respiratory rate of the wearer with the possibility of distinguishing the intensity of the breath. The results presented in this work clearly show the excellent properties of Cell/PANI-PAMPSA as a material for paper electronics, paving the way for new fascinating applications.

CRediT authorship contribution statement

B.B. and I.G. conceived and designed the experiments, and wrote the manuscript; V.M., G.D., and L.Y. performed most of the experiments; I. R., E.B. performed the theoretical calculations; E.S and M.C.C supported in data discussion.

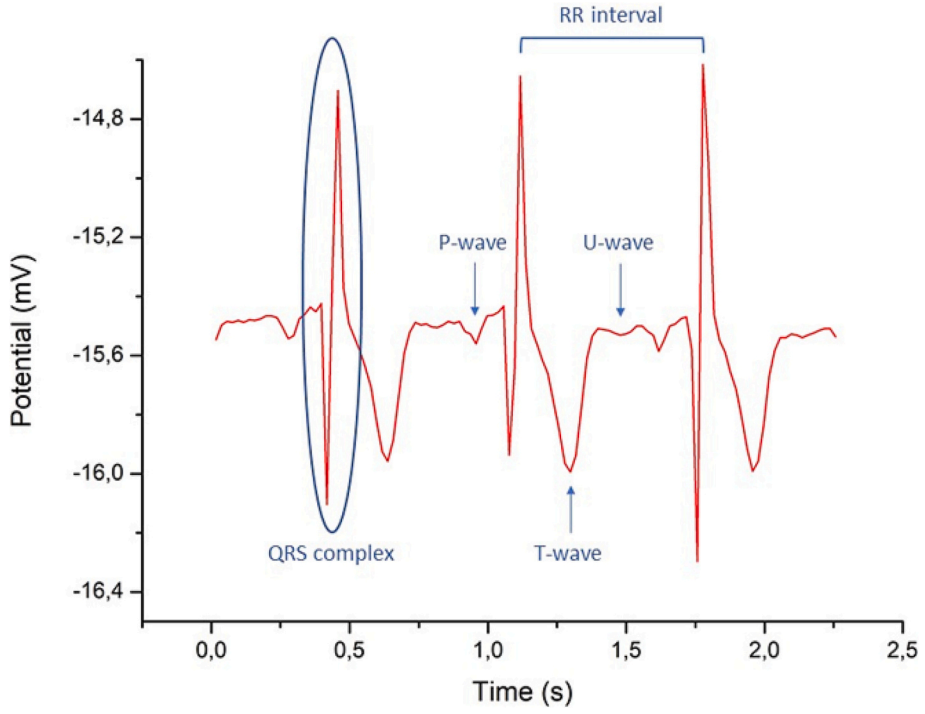

Fig. 9. Output ECG obtained with the Cell/PANI-PAMPSA electrodes; P wave = depolarization of the atria, QRS complex = depolarization of the ventricles, T wave = repolarization of the ventricles, RR interval = time elapsed between two successive R-waves of the QRS signal and U wave = the last phase of ventricular repolarization.

Declaration of competing interest

The authors declare the following financial interests/personal relationships which may be considered as potential competing interests: Barbara Ballarin reports financial support and administrative support were provided by University of Bologna. Barbara Ballarin reports a relationship with University of Bologna that includes: employment. Barbara Ballarin has patent #0 pending to 0. no conflict of interest.

Data availability

Data will be made available on request.

Acknowledgements

The authors wish to thank Dr. Katia Rubini, Department of Chemistry Giacomo Ciamician, UNIBO, for providing the SEM and TGA measurements; Dr. Riccardo Castagnoli for the electrical measurements and Dr. Emanuele Maccaferri, Department of Industrial Chemistry Toso Montanari, for the mechanical tests.

Appendix A. Supplementary data

Electronic Supplementary Information: humidity measurements set-up; sample holder for resistance and mechanical measurements; additional material characterization (TGA; Stress/Strain curves); additional electrical measurements and sensing studies; see DOI: XXXXXXXXX. Supplementary data to this article can be found online at doi:https://doi.org/10.1016/j.carbpol.2023.121079.

References

Acar, G., Ozturk, O., Golparvar, A. J., Elboshra, T. A., Böhringer, K., & Kaya Yapici, M. (2019). Wearable and flexible textile electrodes for biopotential signal monitoring: A review. *Electronics (Switzerland), 8*(5), 1–25. https://doi.org/10.3390/electronics8050479

Al-Ani, M. S. (2018). ECG waveform classification based on P-QRS-T wave recognition. *UHD Journal of Science and Technology, 2*(2), 7–14. https://doi.org/10.21928/uhdjst.v2n2y2018.pp7-14

Al-Halhouli, A., Al-Ghussain, L., Khallouf, O., Rabadi, A., Alawadi, J., Liu, H., … Zheng, D. (2021). Clinical evaluation of respiratory rate measurements on copd (male) patients using wearable inkjet-printed sensor. *Sensors (Switzerland), 21*(2), 1–19. https://doi.org/10.3390/s21020468

Al-Oqla, F. M., Sapuan, S. M., Anwer, T., Jawaid, M., & Hoque, M. E. (2015). Natural fiber reinforced conductive polymer composites as functional materials: A review. *Synthetic Metals, 206*, 42–54. https://doi.org/10.1016/j.synthmet.2015.04.014

Ankhili, A., Tao, X., Cochrane, C., Coulon, D., & Koncar, V. (2018). Washable and reliable textile electrodes embedded into underwear fabric for electrocardiography (ECG) monitoring. *Materials, 11*(2), 1–11. https://doi.org/10.3390/ma11020256

Ankhili, A., Tao, X., Cochrane, C., Koncar, V., Coulon, D., & Tarlet, J. M. (2018). Comparative study on conductive knitted fabric electrodes for long-term electrocardiography monitoring: Silver-plated and PEDOT:PSS coated fabrics. *Sensors (Switzerland), 18*(11). https://doi.org/10.3390/s18113890

Avelar Dutra, F. V., Pires, B. C., Nascimento, T. A., Mano, V., & Borges, K. B. (2017). Polyaniline-deposited cellulose fiber composite prepared via in situ polymerization: Enhancing adsorption properties for removal of meloxicam from aqueous media. *RSC Advances, 7*(21), 12639–12649. https://doi.org/10.1039/c6ra27019k

Barandun, G., Soprani, M., Naficy, S., Grell, M., Kasimatis, M., Chiu, K. L., … Güder, F. (2019). Cellulose fibers enable near-zero-cost electrical sensing of water-soluble gases. *ACS Sensors, 4*(6), 1662–1669. https://doi.org/10.1021/acssensors.9b00555

Bayer, C. L., Trenchard, I. J., & Peppas, N. A. (2010). Analyzing polyaniline-poly(2-acrylamido-2-methylpropane sulfonic acid) biocompatibility with 3T3 fibroblasts. *Journal of Biomaterials Science, Polymer Edition, 21*(5), 623–634. https://doi.org/10.1163/156856209X434647

Boland, C. S., Khan, U., Backes, C., Neill, A. O., Mccauley, J., Duane, S., … Coleman, J. N. (2014). Terms of use bodily motion sensors based on graphene À rubber composites. *ACS Nano, 8*(9), 8819–8830.

Bubniene, U. S., Ratautaite, V., Ramanavicius, A., & Bucinskas, V. (2022). Conducting polymers for the design of tactile sensors. *Polymers, 14*(15), 1–20. https://doi.org/10.3390/polym14152984

Cardoso, M. J. R., Lima, M. F. S., & Lenz, D. M. (2007). Polyaniline synthesized with functionalized sulfonic acids for blends manufacture. *Materials Research, 10*(4), 425–429. https://doi.org/10.1590/S1516-14392007000400017

Castrillón, R., Pérez, J. J., & Andrade-Caicedo, H. (2018). Electrical performance of PEDOT: PSS-based textile electrodes for wearable ECG monitoring: A comparative study. *Biomedical Engineering Online, 17*(1), 1–24. https://doi.org/10.1186/s12938-018-0469-5

Chen, G., Xiao, X., Zhao, X., Tat, T., Bick, M., & Chen, J. (2022). Electronic textiles for wearable point-of-care systems. *Chemical Reviews, 122*(3), 3259–3291. https://doi.org/10.1021/acs.chemrev.1c00502

De Haro-Niza, J., Rincón, E., Gonzalez, Z., Espinosa, E., & Rodríguez, A. (2022). Nanocellulose from Spanish harvesting residues to improve the sustainability and functionality of linerboard recycling processes. *Nanomaterials, 12*(24). https://doi.org/10.3390/nano12244447

Devabaktuni, L., Kulkarni, P. K., Dixit, M., Raavi, P. K., & Krishna, L. N. V. (2015). Sources of cellulose and their applications- A review. *International Journal of Drug Formulation and Research, 2*(January 2011), 19–38.

Duan, Z., Jiang, Y., & Tai, H. (2021). Recent advances in humidity sensors for human body related humidity detection. *Journal of Materials Chemistry C, 9*(42), 14963–14980. https://doi.org/10.1039/d1tc04180k

Fan, J., Zhang, S., Li, F., Yang, Y., & Du, M. (2020). Recent advances in cellulose-based membranes for their sensing applications. *Cellulose, 27*(16), 9157–9179. https://doi.org/10.1007/s10570-020-03445-7

Fei, G., Wang, Y., Wang, H., Ma, Y., Guo, Q., Huang, W., … Ni, Y. (2019). Fabrication of bacterial cellulose/polyaniline nanocomposite paper with excellent conductivity, strength, and flexibility. *ACS Sustainable Chemistry and Engineering, 7*(9), 8215–8225. https://doi.org/10.1021/acssuschemeng.8b06306

Fujita, H., Hao, M., Takeoka, S., Miyahara, Y., Goda, T., & Fujie, T. (2022). Paper-based wearable ammonia gas sensor using organic–inorganic composite PEDOT:PSS with iron(III) compounds. *Advanced Materials Technologies, 7*(8), 1–11. https://doi.org/10.1002/admt.202101486

Grau, G., Kitsomboonloha, R., Swisher, S. L., Kang, H., & Subramanian, V. (2014). Printed transistors on paper: Towards smart consumer product packaging. *Advanced Functional Materials, 24*(32), 5067–5074. https://doi.org/10.1002/adfm.201400129

Gribkova, O. L., Omelchenko, O. D., Trchová, M., Nekrasov, A. A., Ivanov, V. F., Tverskoy, V. A., & Vannikov, A. V. (2013). Preparation of polyaniline in the presence of polymeric sulfonic acids mixtures: The role of intermolecular interactions between polyacids. *Chemical Papers, 67*(8), 952–960. https://doi.org/10.2478/s11696-013-0384-y

Hajlaoui, O., Khiari, R., Ajili, L., Batis, N., & Bergaoui, L. (2020). Design and characterization of type I cellulose-polyaniline composites from various cellulose sources: A comparative study. *Chemistry Africa, 3*(3), 783–792. https://doi.org/10.1007/s42250-020-00148-1

Han, N., Zhang, J., Hoang, M., Gray, S., & Xie, Z. (2021). A review of process and wastewater reuse in the recycled paper industry. *Environmental Technology and Innovation, 24*, Article 101860. https://doi.org/10.1016/j.eti.2021.101860

Han, Z., Li, H., Xiao, J., Song, H., Li, B., Cai, S., … Feng, X. (2019). Ultralow-cost, highly sensitive, and flexible pressure sensors based on carbon black and airlaid paper for wearable electronics. *ACS Applied Materials and Interfaces, 11*(36), 33370–33379. https://doi.org/10.1021/acsami.9b12929

He, P., Cao, J., Ding, H., Liu, C., Neilson, J., Li, Z., … Derby, B. (2019). Screen-printing of a highly conductive graphene ink for flexible printed electronics. *ACS Applied Materials and Interfaces, 11*(35), 32225–32234. https://doi.org/10.1021/acsami.9b04589

He, W., Tian, J., Li, J., Jin, H., & Li, Y. (2016). Characterization and properties of cellulose nanofiber/polyaniline film composites synthesized through in situ polymerization. *BioResources, 11*(4), 8535–8547. https://doi.org/10.15376/biores.11.4.8535-8547

Heikenfeld, J., Jajack, A., Rogers, J., Gutruf, P., Tian, L., Pan, T., Li, R., Khine, M., Kim, J., Wang, J., & Kim, J. (2018). Wearable sensors: Modalities, challenges, and prospects. *Lab on a Chip, 18*(2), 217–248. https://doi.org/10.1039/c7lc00914c

Heller, A., Feldman, B. J., Mano Austin, N., & Yueh-Lin, L. (2016). *Lawyer electron conducting crosslinked polyaniline based redox hydrogel, and method of making* (Patent, US 9,303.279 B2).

Hyun, W. J., Park, O. O., & Chin, B. D. (2013). Foldable graphene electronic circuits based on paper substrates. *Advanced Materials, 25*(34), 4729–4734. https://doi.org/10.1002/adma.201302063

Izadi, A., Hosseini, M., Najafpour Darzi, G., Nabi Bidhendi, G., & Pajoum Shariati, F. (2018). Treatment of paper-recycling wastewater by electrocoagulation using aluminum and iron electrodes. *Journal of Environmental Health Science and Engineering, 16*(2), 257–264. https://doi.org/10.1007/s40201-018-0314-6

Jain, S., Chakane, S., Samui, A. B., Krishnamurthy, V. N., & Bhoraskar, S. V. (2003). Humidity sensing with weak acid-doped polyaniline and its composites. *Sensors and Actuators, B: Chemical, 96*(1–2), 124–129. https://doi.org/10.1016/S0925-4005(03)00511-2

Jeon, J. W., O'Neal, J., Shao, L., & Lutkenhaus, J. L. (2013). Charge storage in polymer acid-doped polyaniline-based layer-by-layer electrodes. *ACS Applied Materials and Interfaces, 5*(20), 10127–10136. https://doi.org/10.1021/am402809e

Jung, Y., Min, J. K., Choi, J., Bang, J., Jeong, S., Pyun, K. R., … Ko, S. H. (2022). Smart paper electronics by laser-induced graphene for biodegradable real-time food spoilage monitoring. *Applied Materials Today, 29*(March), Article 101589. https://doi.org/10.1016/j.apmt.2022.101589

Jung, Y. H., Chang, T. H., Zhang, H., Yao, C., Zheng, Q., Yang, V. W., … Ma, Z. (2015). High-performance green flexible electronics based on biodegradable cellulose nanofibril paper. *Nature Communications, 6*(May). https://doi.org/10.1038/ncomms8170

Kano, S., Jarulertwathana, N., Mohd-noor, S., Hyun, J. K., Asahara, R., & Mekaru, H. (2022). Respiratory monitoring by ultrafast humidity sensors with nanomaterials: A review. *Sensors, 22*(3), 1–30. https://doi.org/10.3390/s22031251

Ke, S., Ouyang, T., Zhang, K., Nong, Y., Mo, Y., Mo, Q., … Cheng, F. (2019). Highly conductive cellulose network/polyaniline composites prepared by wood

fractionation and in situ polymerization of aniline. *Macromolecular Materials and Engineering, 304*(7), 1–10. https://doi.org/10.1002/mame.201900112
Kim, K. K., Hong, S., Cho, H. M., Lee, J., Suh, Y. D., Ham, J., & Ko, S. H. (2015). Highly sensitive and stretchable multidimensional strain sensor with prestrained anisotropic metal nanowire percolation networks. *Nano Letters, 15*(8), 5240–5247. https://doi.org/10.1021/acs.nanolett.5b01505
Kim, Y. H., Moon, D. G., & Han, J. I. (2004). Organic TFT array on a paper substrate. *IEEE Electron Device Letters, 25*(10), 702–704. https://doi.org/10.1109/LED.2004.836502
Kutorglo, E. M., Hassouna, F., Kopecký, D., Fišer, L., Sedlářová, I., Zadražil, A., & Šoóš, M. (2018). Synthesis of conductive macroporous composite polymeric materials using porogen-free method. *Colloids and Surfaces A: Physicochemical and Engineering Aspects, 557*(August 2017), 137–145. https://doi.org/10.1016/j.colsurfa.2017.10.082
Li, Z., Liu, H., Ouyang, C., Hong Wee, W., Cui, X., Jian Lu, T., … Xu, F. (2016). Recent advances in pen-based writing electronics and their emerging applications. *Advanced Functional Materials, 26*(2), 165–180. https://doi.org/10.1002/adfm.201503405
Ling, H., Chen, R., Huang, Q., Shen, F., Wang, Y., & Wang, X. (2020). Transparent, flexible and recyclable nanopaper-based touch sensors fabricated: Via inkjet-printing. *Green Chemistry, 22*(10), 3208–3215. https://doi.org/10.1039/d0gc00658k
Liu, H., Jian, R., Chen, H., Tian, X., Sun, C., Zhu, J., Yang, Z., Sun, J., & Wang, C. (2019). Application of biodegradable and biocompatible nanocomposites in electronics: Current status and future directions. *Nanomaterials, 9*(7). https://doi.org/10.3390/nano9070950
Liu, H., Xiang, H., Wang, Y., Li, Z., Qian, L., Li, P., … Huang, W. (2019). A flexible multimodal sensor that detects strain, humidity, temperature, and pressure with carbon black and reduced graphene oxide hierarchical composite on paper. *ACS Applied Materials and Interfaces, 11*(43), 40613–40619. https://doi.org/10.1021/acsami.9b13349
Miyashiro, D., Hamano, R., & Umemura, K. (2020). A review of applications using mixed materials of cellulose, nanocellulose and carbon nanotubes. *Nanomaterials, 10*(2). https://doi.org/10.3390/nano10020186
Mo, L., Guo, Z., Yang, L., Zhang, Q., Fang, Y., Xin, Z., Chen, Z., Hu, K., Han, L., & Li, L. (2019). Silver nanoparticles based ink with moderate sintering in flexible and printed electronics. *International Journal of Molecular Sciences, 20*(9). https://doi.org/10.3390/ijms20092124
Muchorski, D. (2006). *Tensile properties of paper and paperboard (using constant rate of elongation apparatus). T 494 Om-01. TAPPI* (pp. 1–28).
Muralee Gopi, C. V. V., Vinodh, R., Sambasivam, S., Obaidat, I. M., & Kim, H. J. (2020). Recent progress of advanced energy storage materials for flexible and wearable supercapacitor: From design and development to applications. *Journal of Energy Storage, 27*(November 2019), Article 101035. https://doi.org/10.1016/j.est.2019.101035
Nayak, L., Mohanty, S., Nayak, S. K., & Ramadoss, A. (2019). A review on inkjet printing of nanoparticle inks for flexible electronics. *Journal of Materials Chemistry C, 7*(29), 8771–8795. https://doi.org/10.1039/c9tc01630a
Nepomuceno, N. C., Seixas, A. A. A., Medeiros, E. S., & Mélo, T. J. A. (2021). Evaluation of conductivity of nanostructured polyaniline/cellulose nanocrystals (PANI/CNC) obtained via in situ polymerization. *Journal of Solid State Chemistry, 302*(June). https://doi.org/10.1016/j.jssc.2021.122372
Pang, Z., Yang, Z., Chen, Y., Zhang, J., Wang, Q., Huang, F., & Wei, Q. (2016). A room temperature ammonia gas sensor based on cellulose/TiO2/PANI composite nanofibers. *Colloids and Surfaces A: Physicochemical and Engineering Aspects, 494*, 248–255. https://doi.org/10.1016/j.colsurfa.2016.01.024
Parandeh, S., Kharaziha, M., & Karimzadeh, F. (2019). An eco-friendly triboelectric hybrid nanogenerators based on graphene oxide incorporated polycaprolactone fibers and cellulose paper. *Nano Energy, 59*(February), 412–421. https://doi.org/10.1016/j.nanoen.2019.02.058
Piuzzi, E., Pisa, S., Pittella, E., Podestà, L., & Sangiovanni, S. (2020). Wearable belt with built-in textile electrodes for cardio—Respiratory monitoring. *Sensors (Switzerland), 20*(16), 1–15. https://doi.org/10.3390/s20164500
Ragazzini, I., Gualandi, I., Selli, S., Polizzi, C., Cassani, M. C., Nanni, D., … Ballarin, B. (2021). A simple and industrially scalable method for making a PANI-modified cellulose touch sensor. *Carbohydrate Polymers, 254*(July 2020), Article 117304. https://doi.org/10.1016/j.carbpol.2020.117304
Ragazzini, I., Castagnoli, R., Gualandi, I., Cassani, M. C., Nanni, D., Gambassi, F., … Ballarin, B. (2022). A resistive sensor for humidity detection based on cellulose/polyaniline. *RSC Advances, 12*(43), 28217–28226. https://doi.org/10.1039/d2ra03982f
Rahayu, I., Eddy, D. R., Novianty, A. R., Rukiah, Anggreni, A., Bahti, H., & Hidayat, S. (2019). The effect of hydrochloric acid-doped polyaniline to enhance the conductivity. *IOP Conference Series: Materials Science and Engineering, 509*(1). https://doi.org/10.1088/1757-899X/509/1/012051
Raut, N. C., & Al-Shamery, K. (2018). Inkjet printing metals on flexible materials for plastic and paper electronics. *Journal of Materials Chemistry C, 6*(7), 1618–1641. https://doi.org/10.1039/c7tc04804a
Sabo, R., Yermakov, A., Law, C. T., & Elhajjar, R. (2016). Nanocellulose-enabled electronics, energy harvesting devices, smart materials and sensors: A review. *Journal of Renewable Materials, 4*(5), 297–312. https://doi.org/10.7569/JRM.2016.634114
Say, M. G., Brooke, R., Edberg, J., Grimoldi, A., Belaineh, D., Engquist, I., & Berggren, M. (2020). Spray-coated paper supercapacitors. *Npj Flexible Electronics, 4*(1), 1–7. https://doi.org/10.1038/s41528-020-0079-8
Seddiqi, H., Oliaei, E., Honarkar, H., Jin, J., Geonzon, L. C., Bacabac, R. G., & Klein-Nulend, J. (2021). Cellulose and its derivatives: Towards biomedical applications. In *, Vol. 28, Issue 4. Cellulose*. Netherlands: Springer. https://doi.org/10.1007/s10570-020-03674-w.
Seshadri, D. R., Li, R. T., Voos, J. E., Rowbottom, J. R., Alfes, C. M., Zorman, C. A., & Drummond, C. K. (2019). Wearable sensors for monitoring the physiological and biochemical profile of the athlete. *Npj Digital Medicine, 2*(1). https://doi.org/10.1038/s41746-019-0150-9
Seyedin, M. Z., Razal, J. M., Innis, P. C., & Wallace, G. G. (2014). Strain-responsive polyurethane/PEDOT:PSS elastomeric composite fibers with high electrical conductivity. *Advanced Functional Materials, 24*(20), 2957–2966. https://doi.org/10.1002/adfm.201303905
Sezen-Edmonds, M., Yeh, Y. W., Yao, N., & Loo, Y. L. (2019). Humidity and strain rate determine the extent of phase shift in the piezoresistive response of PEDOT:PSS. *ACS Applied Materials and Interfaces, 11*(18), 16888–16895. https://doi.org/10.1021/acsami.9b00817
Shahadat, M., Khan, M. Z., Rupani, P. F., Embrandiri, A., Sultana, S., Ahammad, S. Z., … Sreekrishnan, T. R. (2017). A critical review on the prospect of polyaniline-grafted biodegradable nanocomposite. *Advances in Colloid and Interface Science, 249* (September), 2–16. https://doi.org/10.1016/j.cis.2017.08.006
Shathi, M. A., Chen, M., Khoso, N. A., Rahman, M. T., & Bhattacharjee, B. (2020). Graphene coated textile based highly flexible and washable sports bra for human health monitoring. *Materials and Design, 193*, Article 108792. https://doi.org/10.1016/j.matdes.2020.108792
Shen, J., Shahid, S., Amura, I., Sarihan, A., Tian, M., & Emanuelsson, E. A. (2018). Enhanced adsorption of cationic and anionic dyes from aqueous solutions by polyacid doped polyaniline. *Synthetic Metals, 245*(June), 151–159. https://doi.org/10.1016/j.synthmet.2018.08.015
Tobjörk, D., & Österbacka, R. (2011). Paper electronics. *Advanced Materials, 23*(17), 1935–1961. https://doi.org/10.1002/adma.201004692
Wang, J., Su, W., Zhang, J., Zhou, A., Bai, H., & Zhang, T. (2021). Improving the volumetric specific capacitance of flexible polyaniline electrode: Solution casting method and effect of reduced graphene oxide sheets. *Science China Materials, 64*(3), 571–580. https://doi.org/10.1007/s40843-020-1472-3
Wang, Y., Yan, C., Cheng, S. Y., Xu, Z. Q., Sun, X., Xu, Y. H., … Feng, Z. S. (2019). Flexible RFID tag metal antenna on paper-based substrate by inkjet printing technology. *Advanced Functional Materials, 29*(29). https://doi.org/10.1002/adfm.201902579
Webster, J. (2010). *Medical instrumentation: Application and design* (4th ed., pp. 590–606). John Wiley and Sons, Inc. USA.
Wu, M., Li, Y., An, N., & Sun, J. (2016). Applied voltage and near-infrared light enable healing of superhydrophobicity loss caused by severe scratches in conductive superhydrophobic films. *Advanced Functional Materials, 26*(37), 6777–6784. https://doi.org/10.1002/adfm.201601979
Yamamoto, Y., Yamamoto, D., Takada, M., Naito, H., Arie, T., Akita, S., & Takei, K. (2017). Efficient skin temperature sensor and stable gel-less sticky ECG sensor for a wearable flexible healthcare patch. *Advanced Healthcare Materials, 6*(17), 1–7. https://doi.org/10.1002/adhm.201700495
Yang, L., Wang, H., Yuan, W., Li, Y., Gao, P., Tiwari, N., … Cheng, H. (2021). Wearable pressure sensors based on MXene/tissue papers for wireless human health monitoring. *ACS Applied Materials and Interfaces, 13*(50), 60531–60543. https://doi.org/10.1021/acsami.1c22001
Yang, Y., Huang, Q., Payne, G. F., Sun, R., & Wang, X. (2019). A highly conductive, pliable and foldable Cu/cellulose paper electrode enabled by controlled deposition of copper nanoparticles. *Nanoscale, 11*(2), 725–732. https://doi.org/10.1039/c8nr07123c
Yapici, M. K., & Alkhidir, T. E. (2017). Intelligent medical garments with graphene-functionalized smart-cloth ECG sensors. *Sensors (Switzerland), 17*(4), 1–12. https://doi.org/10.3390/s17040875
Yoo, J. E., & Bae, J. (2013). The influence of aniline to acid composition on the electrical conductivity of pani-paampsa. *Bulletin of the Korean Chemical Society, 34*(12), 3825–3828. https://doi.org/10.5012/bkcs.2013.34.12.3825
Yoo, J. E., Cross, J. L., Bucholz, T. L., Lee, K. S., Espe, M. P., & Loo, Y. L. (2007). Improving the electrical conductivity of polymer acid-doped polyaniline by controlling the template molecular weight. *Journal of Materials Chemistry, 17*(13), 1268–1275. https://doi.org/10.1039/b618521e
Zhang, X., Zhu, J., Haldolaarachchige, N., Ryu, J., Young, D. P., Wei, S., & Guo, Z. (2012). Synthetic process engineered polyaniline nanostructures with tunable morphology and physical properties. *Polymer, 53*(10), 2109–2120. https://doi.org/10.1016/j.polymer.2012.02.042
Zhang, Y., Zhang, L., Cui, K., Ge, S., Cheng, X., Yan, M., Yu, J., & Liu, H. (2018). Flexible electronics based on micro/nanostructured paper. *Advanced Materials, 30*(51), 1–39. https://doi.org/10.1002/adma.201801588
Zhao, H., Zhang, T., Qi, R., Dai, J., Liu, S., & Fei, T. (2017). Drawn on paper: A reproducible humidity sensitive device by handwriting. *ACS Applied Materials and Interfaces, 9*(33), 28002–28009. https://doi.org/10.1021/acsami.7b05181
Zhao, P., Zhang, R., Tong, Y., Zhao, X., Tang, Q., & Liu, Y. (2020). All-paper, all-organic, cuttable, and foldable pressure sensor with tuneable conductivity polypyrrole. *Advanced Electronic Materials, 6*(8), 1–10. https://doi.org/10.1002/aelm.201901426
Zhen, L. W., Thai, Q. B., Nguyen, T. X., Le, D. K., Lee, J. K. W., Xiang, Y. Q., & Duong, H. M. (2019). Recycled cellulose aerogels from paper waste for a heat insulation design of canteen bottles. *Fluids, 4*(3), 1–9. https://doi.org/10.3390/nn4030174